

# Brønsted basicity of the air–water interface

Himanshu Mishra<sup>a,b,c</sup>, Shinichi Enami<sup>d,e,f</sup>, Robert J. Nielsen<sup>c</sup>, Logan A. Stewart<sup>g</sup>, Michael R. Hoffmann<sup>a</sup>, William A. Goddard III<sup>b,c</sup>, and Agustín J. Colussi<sup>a,1</sup>

<sup>a</sup>Ronald and Maxine Linde Center for Global Environmental Science, <sup>b</sup>Materials Science Department, and <sup>c</sup>Materials and Process Simulation Center, California Institute of Technology, Pasadena, CA 91125; <sup>d</sup>The Hakubi Center for Advanced Research, Kyoto University, Kyoto 606-8302, Japan; <sup>e</sup>Research Institute for Sustainable Humanosphere, Kyoto University, Uji 611-0011, Japan; <sup>f</sup>Precursory Research for Embryonic Science and Technology, Japan Science and Technology Agency, Kawaguchi 332-0012, Japan; and <sup>g</sup>Physics Department, University of California, Santa Barbara, Santa Barbara, CA 93106

Edited by Michael L. Klein, Temple University, Philadelphia, PA, and approved October 2, 2012 (received for review June 1, 2012)

Differences in the extent of protonation of functional groups lying on either side of water–hydrophobe interfaces are deemed essential to enzymatic catalysis, molecular recognition, bioenergetic transduction, and atmospheric aerosol–gas exchanges. The sign and range of such differences, however, remain conjectural. Herein we report experiments showing that gaseous carboxylic acids RCOOH(g) begin to deprotonate on the surface of water significantly more acidic than that supporting the dissociation of dissolved acids RCOOH(aq). Thermodynamic analysis indicates that > 6 H<sub>2</sub>O molecules must participate in the deprotonation of RCOOH(g) on water, but quantum mechanical calculations on a model air–water interface predict that such event is hindered by a significant kinetic barrier unless OH<sup>−</sup> ions are present therein. Thus, by detecting RCOO<sup>−</sup> we demonstrate the presence of OH<sup>−</sup> on the aerial side of on pH > 2 water exposed to RCOOH(g). Furthermore, because in similar experiments the base (Me)<sub>3</sub>N(g) is protonated only on pH < 4 water, we infer that the outer surface of water is Brønsted neutral at pH ~3 (rather than at pH 7 as bulk water), a value that matches the isoelectric point of bubbles and oil droplets in independent electrophoretic experiments. The OH<sup>−</sup> densities sensed by RCOOH(g) on the aerial surface of water, however, are considerably smaller than those at the (>1 nm) deeper shear planes probed in electrophoresis, thereby implying the existence of OH<sup>−</sup> gradients in the interfacial region. This fact could account for the weak OH<sup>−</sup> signals detected by surface-specific spectroscopies.

gas–liquid reactions | surface potential | water surface acidity | interfacial proton transfer

**A**cid–base chemistry at aqueous interfaces lies at the heart of major processes in chemistry and biology. Changes in the degree of dissociation of the acidic/basic residues upon translocation between aqueous and hydrophobic microenvironments orchestrate enzyme catalysis (1), drive proton/electron transport across biomembranes (2, 3), and mediate molecular recognition and self-assembly phenomena (4–6). Despite its importance, the characterization of acid–base chemistry at aqueous interfaces remains fraught with uncertainties (7–11). Basic questions linger about the thickness of interfacial layers (12), how acidity changes through the interfacial region (13), and the mechanistic differences between proton transfer (PT) across interfacial (IF) versus in bulk (B) water (10, 14). Because aqueous surfaces are usually charged relative to the bulk liquid (15), the thermodynamic requirement of uniform electrochemical activity throughout (including the interfacial regions) implies that the chemical activity of protons (pH) in IF could be different from that in the B liquid. Reduced hydration of ionic species at the interface could force acids and bases toward their undissociated forms (16).

These fundamental issues have been extensively investigated via electrostatic (17) and electrokinetic experiments (11), surface tension studies and analysis (18, 19), surface-specific spectroscopies (9, 20–22), and theoretical (quantum mechanical and molecular dynamics) calculations (7, 23–25). Some experimental (9) and theoretical (7, 25, 26) results were interpreted to signify that the air–water interface is more acidic than bulk water, whereas others reached the opposite conclusion (8, 11, 21, 23,

27). The impasse stems in part from the failure to recognize that acidity is a relative concept describing the extent of proton sharing between two conjugate acid/base pairs under specified conditions. Theoretical calculations and surface-specific spectroscopies on the structure of interfacial water are therefore moot about its functional acidity. By definition (28), W is a Brønsted base if and only if it can accept protons from Brønsted acids AH, reaction R1



An operational measure of the basicity of W as a medium is given by the acidity constant of AH therein:  $K_A = [\text{A}^-][\text{WH}^+]/[\text{AH}]$ . If W is bulk water, the acidity constant  $K_{A,B}$  can be derived from experimental data on the degree of dissociation:  $\theta_B = [\text{A}^-]/([\text{A}^-] + [\text{AH}])$ , as a function of pH via Eq. 1,

$$\theta_B = 1/(1 + 10^{\text{p}K_A - \text{pH}}) \quad [\text{1}]$$

A formal extension of Eq. 1 to interfacial water would require ( $\theta_{\text{IF}}$ ,  $\text{pH}_{\text{IF}}$ ) rather than experimentally accessible ( $\theta_{\text{IF}}$ , pH) data. This is an essential difficulty because the estimation of  $\text{pH}_{\text{IF}}$  from  $\text{pH}_B$  (16, 29) necessarily involves assumptions about ion distributions and the dielectric properties of water in double layers of molecular dimensions (30–33) (SI Discussion). Lacking a thermodynamic  $\text{pH}_{\text{IF}}$  scale based on independent measurements, interfacial acidity constants  $K_{A,\text{IF}}$  become constructs circularly defined from estimated  $\text{pH}_{\text{IF}}$  values. These simple considerations should make it apparent that conventional concepts on acidity in bulk phases may be meaningless in connection with interfaces.

It is, however, meaningful to ask whether the Brønsted basicity of water is different on either side of water–hydrophobe interfaces. Here we sought to answer this question by performing appropriate experiments. Experiments had to ensure that the acidic probe, AH, would exchange its proton with the interface immediately before the detection of ( $\text{A}^- + \text{XH}^+$ ) products. Mapping interfacial layers of molecular thicknesses further calls for static molecular probes locked at specified depths, or dynamic ones that interact with the interface during intervals shorter than characteristic diffusion times through the interfacial region. Below, we report experiments in which the production of  $\text{A}^-$  is monitored as a function of pH via online electrospray ionization mass spectrometry (ESI-MS) of the interfacial layers of injected aqueous jets containing dissolved AH(aq) versus those collided with gaseous AH(g) molecules (Fig. S1 and SI Methods) (10, 34). The decisive advantages of online mass spectrometry over spectro-

Author contributions: H.M., S.E., R.J.N., and L.A.S. performed research; H.M., S.E., R.J.N., L.A.S., W.A.G., and A.J.C. analyzed data; M.R.H. contributed new reagents/analytic tools; A.J.C. designed research; and A.J.C. wrote the paper.

The authors declare no conflict of interest.

This article is a PNAS Direct Submission.

<sup>1</sup>To whom correspondence should be addressed. E-mail: ajcolussi@caltech.edu.

This article contains supporting information online at [www.pnas.org/lookup/suppl/doi:10.1073/pnas.1209307109/-DCSupplemental](http://www.pnas.org/lookup/suppl/doi:10.1073/pnas.1209307109/-DCSupplemental).







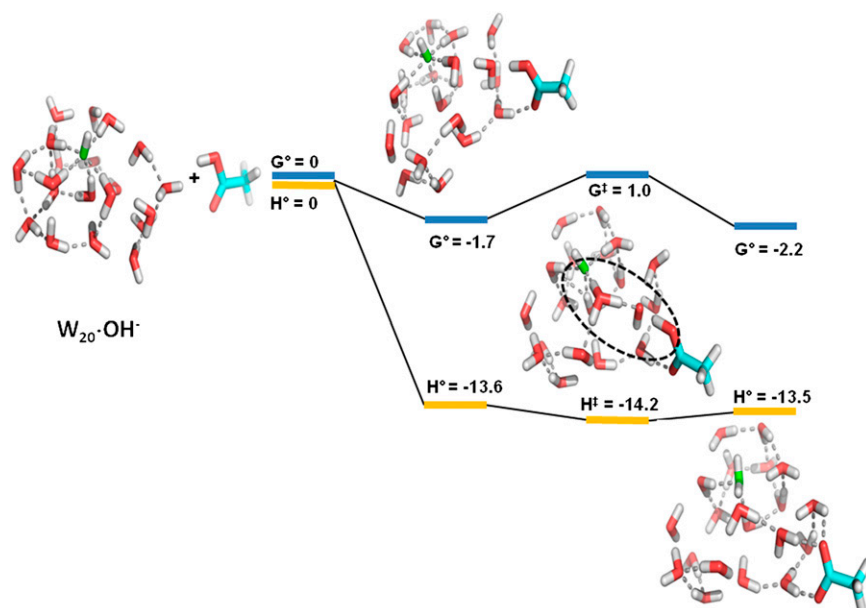


**Fig. 3.** Calculated Gibbs free energies ( $G^\circ$ ) and enthalpies ( $H^\circ$ ) (in  $\text{kcal}\cdot\text{mol}^{-1}$ ) of reactants, adducts, transition states, and products of optimized water clusters containing hydroxide,  $W_{20}\cdot\text{OH}^-$  in contact with acetic acid. Calculations in the absence of  $\text{OH}^-$  did not yield stable  $[\text{CH}_3\text{COO}^- + \text{H}_3\text{O}^+]$  dissociation products.

to exchange protons with other entities under specific conditions and, therefore, strictly apply to chemical reactions rather than to structural features.

The finding that the charge density on the aerial side of the interface,  $\sigma_{\text{qOH}}$ , estimated from our reactive gas–liquid experiments is considerably smaller than that detected at the shear hydrodynamic plane,  $\sigma_\zeta$ , suggests the existence of nonmonotonic  $\text{OH}^-$  vertical profiles. We have recently shown that different anions populate interfacial layers at depths that are inversely correlated with their relative surface affinities (63). The emerging picture is that surface affinities indicate how close anions approach the interface rather than their relative concentrations within a single subsurface layer. Thus, the possibility arises that ion concentration profiles within interfacial double layers could be nonmonotonic (31) and, as a result, experiments probing water basicity at different depths could lead to dissimilar results. One corollary is that the low affinity of  $\text{OH}^-$  for the air–water interface predicated by some calculations (7, 25) and implied by some surface-specific spectroscopies (9) is not in principle incompatible with the sizable charge densities deduced from electrophoretic experiments (8). Note that these arguments are conditional, because the reported electrophoretic  $\sigma_\zeta$  values are derived from experimental  $\zeta$ -potentials by using a continuous Gouy–Chapman model for the double layer based on the dielectric constant of bulk water (31, 32) and are, as such, susceptible to major revision.

Because our experimental results are based on sampling the composition of the surface of nascent water jets exposed to  $\text{RCOOH}(\text{g})$  within a few tens of microseconds after emerging from the nozzle, whereas electrophoretic experiments involve much longer time scales, the finding that  $\text{pH}_{\text{PZC}} \sim \text{pI}$  seems to suggest that equilibrium is established in both cases. Note however that the  $\text{OH}^-$  ions populating the air–water interfaces monitored in our experiments must then be produced at faster rates than those estimated from the dissociation of bulk water:  $2\text{H}_2\text{O} = \text{H}_3\text{O}^+ + \text{OH}^-$ , whose characteristic times:  $\tau_{\text{dissociation}} = k_{\text{forward}}^{-1} = (K_w k_{\text{backward}})^{-1} \sim (10^{-14} \times 10^{11} \text{ M}^{-1}\cdot\text{s}^{-1})^{-1} = 10^3 \text{ s}$  (64, 65), vastly exceed the lifetimes of our water jets (7). Water autolysis concurrent with  $\text{OH}^-$  diffusion and binding at the interface may effectively shorten relaxation times into the submillisecond

timescale (54), but other explanations are possible (66). This important issue is being investigated in our laboratory.

To sum up, we (i) demonstrate the presence of hydroxide ions on the aerial surface of  $\text{pH} > 2$  water, (ii) ascribe the negative charge of the surface of neat water to excess  $\text{OH}^-$ , (iii) infer the existence of nonmonotonic  $\text{OH}^-$  profiles through interfacial water layers, and (iv) determine a point of zero charge  $\text{pH}_{\text{PZC}} \sim 3$  for water–hydrophobe interfaces that is consistent with the value obtained in the electrophoresis of bubbles and oil droplets.

## Methods

**Experimental Procedures.** Gas–liquid experiments were conducted by intersecting free-flowing aqueous jets with  $\text{C}_5\text{H}_{11}\text{COOH}(\text{g})/\text{N}_2(\text{g})$  beams in a chamber held at 1 atm, 293 K, and detecting the formation of  $\text{C}_5\text{H}_{11}\text{COO}^-$  therein via online ESI-MS. Our ESI mass spectrometer, which has been described in detail elsewhere (10, 14, 34), is configured to report the ion composition of the net charges generated from the fragmentation of the primary drops sheared from the jet by a fast coaxial annular nebulizer gas flow (67, 68). This claim has been previously validated by showing that (i) the relative anion abundances at air–water interface, i.e., the mass-spectral signal intensities, measured on aqueous jets consisting of equimolar solutions of mixed salts follow a normal Hofmeister series (as expected at the air–water interface and confirmed by other surface-sensitive techniques) and are specifically affected by cationic or anionic surfactants (36), (ii) mass spectra of aqueous jets exposed to reactive gases detect species necessarily produced at the gas–liquid interface rather than in bulk water. For further details see *SI Methods*.

**Computational Details.** Gibbs free energies ( $G$ ) at 298 K were computed from calculated enthalpies ( $H$ ) and entropies ( $S$ ) according to  $G = E_{\text{elec}} + \text{ZPE} + H_{\text{vib}} - TS_{\text{vib}}$ . Geometries of energy minima states were optimized using the M06 functional (44) and 6-311G\*\* basis (69) for all atoms. After geometry optimization, the electronic energy  $E_{\text{elec}}$  was evaluated with the 6-311G\*\*++ basis (70). The Hessians at these geometries were used to determine that the minima and transition states led to 0 and 1 imaginary frequency, respectively. Vibrational frequencies provided zero-point energies and vibrational contributions to enthalpies and entropies. The free energies of acetic acid at 1 atm were calculated using statistical mechanics for ideal gases.

**ACKNOWLEDGMENTS.** Our research is supported by Japan Society for the Promotion of Sciences Postdoctoral Fellowship for Research Abroad (to S.E.) and National Science Foundation Grant AGS-964842a (to M.R.H.).

- Warshel A, et al. (2006) Electrostatic basis for enzyme catalysis. *Chem Rev* 106(8): 3210–3235.
- Mulkidjanian AY, Heberle J, Cherepanov DA (2006) Protons @ interfaces: Implications for biological energy conversion. *Biochim Biophys Acta Bioenerg* 1757:913–930.
- Sandén T, Salomonsson L, Brzezinski P, Widengren J (2010) Surface-coupled proton exchange of a membrane-bound proton acceptor. *Proc Natl Acad Sci USA* 107(9): 4129–4134.
- Bell RC, Wu K, Iedema MJ, Schenter GK, Cowin JP (2009) The oil-water interface: Mapping the solvation potential. *J Am Chem Soc* 131(3):1037–1042.
- Ariga K, Nakanishi T, Hill JP (2006) A paradigm shift in the field of molecular recognition at the air-water interface: From static to dynamic. *Soft Matter* 2(6):465–477.
- McGorty R, Fung J, Kaz D, Manoharan VN (2010) Colloidal self-assembly at an interface. *Mater Today* 13:34–42.
- Buch V, Milet A, Vácha R, Jungwirth P, Devlin JP (2007) Water surface is acidic. *Proc Natl Acad Sci USA* 104(18):7342–7347.
- Beattie JK, Djerdjev AM, Warr GG (2009) The surface of neat water is basic. *Faraday Discuss* 141:31–39, and discussion 81–98.
- Petersen PB, Saykally RJ (2008) Is the liquid water surface basic or acidic? Macroscopic vs. molecular-scale investigations. *Chem Phys Lett* 458:255–261.
- Enami S, Hoffmann MR, Colussi AJ (2010) Proton availability at the air/water interface. *J Phys Chem Lett* 1:1599–1604.
- Marinova KG, et al. (1996) Charging of oil-water interfaces due to spontaneous adsorption of hydroxyl ions. *Langmuir* 12:2045–2051.
- Stiopin IV, et al. (2011) Hydrogen bonding at the water surface revealed by isotopic dilution spectroscopy. *Nature* 474(7350):192–195.
- Mulkidjanian AY (2006) Proton in the well and through the desolvation barrier. *Biochim Biophys Acta* 1757(5-6):415–427.
- Mishra H, et al. (2012) Anions dramatically enhance proton transfer through aqueous interfaces. *Proc Natl Acad Sci USA* 109(26):10228–10232.
- Fawcett WR (2008) The ionic work function and its role in estimating absolute electrode potentials. *Langmuir* 24(17):9868–9875.
- Zhao XL, Subrahmanyam S, Eiselthal KB (1990) Determination of  $pK_a$  at the air/water interface by second harmonic generation. *Chem Phys Lett* 171:558–562.
- Jarvis NL, Scheiman MA (1968) Surface potentials of aqueous electrolyte solutions. *J Phys Chem* 72:74–80.
- Petersen PB, Saykally RJ (2005) Adsorption of ions to the surface of dilute electrolyte solutions: The Jones-Ray effect revisited. *J Am Chem Soc* 127(44):15446–15452.
- Pegram LM, Record MT (2008) Quantifying accumulation or exclusion of  $H^+$ ,  $HO^-$ , and Hofmeister salt ions near interfaces. *Chem Phys Lett* 467:1–8.
- Tian CS, Ji N, Waychunas GA, Shen YR (2008) Interfacial structures of acidic and basic aqueous solutions. *J Am Chem Soc* 130(39):13033–13039.
- Tian CS, Shen YR (2009) Structure and charging of hydrophobic material/water interfaces studied by phase-sensitive sum-frequency vibrational spectroscopy. *Proc Natl Acad Sci USA* 106(36):15148–15153.
- Byrnes SJ, Geissler PL, Shen YR (2011) Ambiguities in surface nonlinear spectroscopy calculations. *Chem Phys Lett* 516:115–124.
- Gray-Weale A, Beattie JK (2009) An explanation for the charge on water's surface. *Phys Chem Chem Phys* 11(46):10994–11005.
- Kudin KN, Car R (2008) Why are water-hydrophobic interfaces charged? *J Am Chem Soc* 130(12):3915–3919.
- Iuchi S, Chen HN, Paesani F, Voth GA (2009) Hydrated excess proton at water-hydrophobic interfaces. *J Phys Chem B* 113(13):4017–4030.
- Vácha R, Buch V, Milet A, Devlin JP, Jungwirth P (2007) Autoionization at the surface of neat water: Is the top layer pH neutral, basic, or acidic? *Phys Chem Chem Phys* 9(34):4736–4747.
- Zangi R, Engberts JBFN (2005) Physisorption of hydroxide ions from aqueous solution to a hydrophobic surface. *J Am Chem Soc* 127(7):2272–2276.
- Nic M, Jirat J, Kosata B, Jenkins A (2006) *IUPAC Compendium of Chemical Terminology* (Blackwell Scientific, Oxford).
- Zhao XL, Ong SW, Wang HF, Eiselthal KB (1993) New method for determination of surface  $pK_a$  using 2<sup>nd</sup> harmonic generation. *Chem Phys Lett* 214:203–207.
- Rowlinson JS, et al. (1981) Structure of the interfacial region—General discussion. *Faraday Symp Chem Soc* 5:16:205–256.
- Luo GM, et al. (2006) Ion distributions near a liquid-liquid interface. *Science* 311(5758):216–218.
- Netz RR, Orland H (2000) Beyond Poisson-Boltzmann: Fluctuation effects and correlation functions. *Eur Phys J E* 1:203–214.
- Cherepanov DA (2004) Force oscillations and dielectric overscreening of interfacial water. *Phys Rev Lett* 93(26):266104–1–266104-4.
- Enami S, Stewart LA, Hoffmann MR, Colussi AJ (2010) Superacid chemistry on mildly acidic water. *J Phys Chem Lett* 1:3488–3493.
- Cheng J, Hoffmann MR, Colussi AJ (2008) Anion fractionation and reactivity at air/water: Methanol interfaces. Implications for the origin of Hofmeister effects. *J Phys Chem B* 112(24):7157–7161.
- Cheng J, Vecitis CD, Hoffmann MR, Colussi AJ (2006) Experimental anion affinities for the air/water interface. *J Phys Chem B* 110(51):25598–25602.
- Enami S, Hoffmann MR, Colussi AJ (2008) Acidity enhances the formation of a persistent ozonide at aqueous ascorbate/ozone gas interfaces. *Proc Natl Acad Sci USA* 105(21):7365–7369.
- Haynes WM (2012) *Handbook of Chemistry and Physics* (Taylor and Francis, London).
- Hunter EPL, Lias SG (1998) Evaluated gas phase basicities and proton affinities of molecules: An update. *J Phys Chem Ref Data* 27:413–656.
- Meot-Ner M (2005) The ionic hydrogen bond. *Chem Rev* 105(1):213–284.
- Leopold KR (2011) Hydrated acid clusters. *Annu Rev Phys Chem* 62:327–349.
- Nguyen S, Fenn JB (2007) Gas-phase ions of solute species from charged droplets of solutions. *Proc Natl Acad Sci USA* 104(4):1111–1117.
- Park JM, Laio A, Iannuzzi M, Parrinello M (2006) Dissociation mechanism of acetic acid in water. *J Am Chem Soc* 128(35):11318–11319.
- Zhao Y, Truhlar DG (2008) The M06 suite of density functionals for main group thermochemistry, thermochemical kinetics, noncovalent interactions, excited states, and transition elements: Two new functionals and systematic testing of four M06-class functionals and 12 other functionals. *Theor Chem Acc* 120:215–241.
- Bryantsev VS, Diallo MS, van Duin ACT, Goddard WA (2009) Evaluation of B3LYP, X3LYP, and M06-class density functionals for predicting the binding energies of neutral, protonated, and deprotonated water clusters. *J Chem Theory Comput* 5: 1016–1026.
- Mishra H, Nielsen RJ, Enami S, Hoffmann MR, Goddard WA III, Colussi AJ (2012) Quantum chemical insights into the dissociation of nitric acid on the surface of aqueous electrolytes. *Int J Theor Chem*, 10.1002/qua.24151.
- Maheshwary S, Patel N, Sathyamurthy N, Kulkarni AD, Gadre SR (2001) Structure and stability of water clusters  $(H_2O)_n$ ,  $n = 8-20$ : An ab initio investigation. *J Phys Chem A* 105:10525–10537.
- Otten DE, Shaffer PR, Geissler PL, Saykally RJ (2012) Elucidating the mechanism of selective ion adsorption to the liquid water surface. *Proc Natl Acad Sci USA* 109(3): 701–705.
- Grimme S (2006) Semiempirical GGA-type density functional constructed with a long-range dispersion correction. *J Comput Chem* 27(15):1787–1799.
- Dahlke EE, Truhlar DG (2005) Improved density functionals for water. *J Phys Chem B* 109(33):15677–15683.
- Mundy CJ, Kuo IFW, Tuckerman ME, Lee HS, Tobias DJ (2009) Hydroxide anion at the air-water interface. *Chem Phys Lett* 481:2–8.
- Jungwirth P, Tobias DJ (2006) Specific ion effects at the air/water interface. *Chem Rev* 106(4):1259–1281.
- Takahashi M (2005)  $\zeta$  potential of microbubbles in aqueous solutions: Electrical properties of the gas-water interface. *J Phys Chem B* 109(46):21858–21864.
- Liu M, Beattie JK, Gray-Weale AA (2012) The surface relaxation of water. *J Phys Chem B* 116(30):8981–8988.
- Vácha R, et al. (2011) The orientation and charge of water at the hydrophobic oil droplet-water interface. *J Am Chem Soc* 133(26):10204–10210.
- Ben-Amotz D (2011) Unveiling electron promiscuity. *J Phys Chem Lett* 2:1216–1222.
- Kuhne TD, Pascal TA, Kaxiras E, Jung Y (2011) New insights into the structure of the vapor/water interface from large-scale first-principles simulations. *J Phys Chem Lett* 2: 105–113.
- Vácha R, et al. (2012) Charge transfer between water molecules as the possible origin of the observed charging at the surface of pure water. *J Phys Chem Lett* 3:107–111.
- Zhan CG, Dixon DA (2003) The nature and absolute hydration free energy of the solvated electron in water. *J Phys Chem B* 107:4403–4417.
- Buchner F, Schultz T, Lübcke A (2012) Solvated electrons at the water-air interface: Surface versus bulk signal in low kinetic energy photoelectron spectroscopy. *Phys Chem Chem Phys* 14(16):5837–5842.
- Petersen PB, Saykally RJ (2006) Probing the interfacial structure of aqueous electrolytes with femtosecond second harmonic generation spectroscopy. *J Phys Chem B* 110(29):14060–14073.
- Takahashi H, et al. (2011) Energetic origin of proton affinity to the air/water interface. *J Phys Chem B* 115(16):4745–4751.
- Enami S, Mishra H, Hoffmann MR, Colussi AJ (2012) Hofmeister effects in micromolar electrolyte solutions. *J Chem Phys* 136(15):154707–1–154707-5.
- Geissler PL, Dellago C, Chandler D, Hutter J, Parrinello M (2001) Autoionization in liquid water. *Science* 291(5511):2121–2124.
- Hassanali A, Prakash MK, Eshet H, Parrinello M (2011) On the recombination of hydronium and hydroxide ions in water. *Proc Natl Acad Sci USA* 108(51):20410–20415.
- Donten ML, Vandevondele J, Hamm P (2012) Speed limits for acid-base chemistry in aqueous solutions. *Chimia (Aarau)* 66(4):182–186.
- Theofanous TG, et al. (2012) The physics of aerobreakup. II. Viscous liquids. *Phys Fluids* 24:022104-1–022104-39.
- Zilch LW, Maze JT, Smith JW, Ewing GE, Jarrold MF (2008) Charge separation in the aerodynamic breakup of micrometer-sized water droplets. *J Phys Chem A* 112(51): 13352–13363.
- Franci MM, et al. (1982) Self-consistent molecular-orbital methods. 23. A polarization-type basis set for 2<sup>nd</sup> row elements. *J Chem Phys* 77:3654–3665.
- Clark T, Chandrasekhar J, Spitznagel GW, Schleyer PV (1983) Efficient diffuse function-augmented basis sets for anion calculations. 3. The 3-21+G basis set for 1<sup>st</sup> row elements, Li-F. *J Comput Chem* 4:294–301.